Journal of Cultural Heritage 43 (2020) 144–152

Available online at
ScienceDirect
www.sciencedirect.com

Elsevier Masson France
EM|consulte
www.em-consulte.com/en

Original article

Influence of the geometric model on the structural analysis of architectural heritage

Domenico Giaccone*, Pierluigi Fanelli, Ulderico Santamaria

Dipartimento di Economia, Impresa e Società, Università degli Studi della Tuscia, via S. Camillo de Lellis, s.n., 01100 Viterbo, Italy

ARTICLE INFO

Article history:
Received 25 June 2019
Accepted 5 December 2019
Available online 17 January 2020

Keywords:
Architectural heritage
Stone column
Finite element analysis
Geometric model
Viterbo

ABSTRACT

Geometric models employed for structural analyses are usually strongly simplified, in order to make easier and faster the numerical solving. Sometimes this approach is valid and convenient as far as it does not influence the analysis results. However, depending on the circumstances and the objectives of the analysis, the model has to be accurately and precisely represented to capture the necessary outputs. This is the case with architectural heritage. In fact, in this field, the surveyed objects are often characterised by complex forms and remarkable damages, which can affect the geometry significantly. Nowadays, many techniques are available to obtain very detailed models of the surface of the object, but they do not allow to consider also interior damages or the constructive features. This information can be obtained through a careful knowledge and anamnesis of the object to study, based on visual inspection and instrumental measures. In this way, the creation of the model to undergoes to a structural analysis, consists in a synthetic operation conducted by the operator in a conscious way. This paper aims to prove that the results of a structural analyses can change significantly, depending on the accuracy and the level of detail of the model. The study was conducted on a basic building element, that is a column, really existing and belonging to a monumental fountain. The column was modelled in five different ways which differ in the level of detail. An ultrasonic test was conducted on the real object to characterise cracks which were taken into account in the most accurate models. A comparison among the five models was done from a static and dynamic perspective, through the following analyses: static, buckling, modal and dynamic with response spectrum.

1. Introduction

1.1. Geometric models in structural analysis

Structural assessment is based on the definition of an analytical model, that is a design scheme which takes into account geometry, constrains and loads. According to the aim of the assessment itself, the analytical model can be more or less real. This means that the surveying object undergoes a simplification process which is conducted by the operator and so, influenced by his skill and sensitivity.

Simple models have been always preferred because they allow to make easier and faster the numerical solving of the structural problems. This approach is widely followed also in the field of architectural heritage, despite complexities which characterise the surveyed objects can reduce the reliability of the model and invalidate the results. For instance, it has been recently used by Boscato et al., for the modelling of multi-leaf masonry walls damaged and consolidated [1]. Complexities which affect the architectural heritage can be of different kind. They can be related to the geometry, the construction materials and techniques, and they can also derive from damages which modify the original shape of the building elements, such as static displacements, deformations, cracks, and loose of parts.

Nowadays, a lot of computer programmes allow to make reliable 3D models of the surveyed object to use in reverse engineering modelling applications. For instance, Lidar (Light Detection and Ranging or Laser Imaging Detection and Ranging) and photogrammetry are two of the most known and widespread techniques, used to do it. They allow to obtain very realistic models of the surveyed object with a great accuracy. Typical applications consist on the inventory of buildings which are in good conditions, and the assessment of the building deflections [2] or the out-of-plane of building elements (i.e. the façade) [3]. Moreover, they are especially appreciated in organic un-rational contexts [4], that is when the investigated object cannot be described through the rules of the Euclidean geometry, in archaeological contexts [5,6] and in

Abbreviations: FEA, finite element analysis; US, ultrasonic.

* Corresponding author.
E-mail addresses: d.giaccone@unitus.it (D. Giaccone), pierluigi.fanelli@unitus.it (P. Fanelli), santamaria@unitus.it (U. Santamaria).

https://doi.org/10.1016/j.culher.2019.12.001
1296-2074/

damaged areas, such as the historical centres interested by earthquakes [7].

However, these tools have some drawback which limit their usefulness in structural assessment. As regards the geometry of the surveyed object, they do not allow to recognise either cracks and voids which could be under the surface, or undercut zones, which occur when the object is complex and cannot be easily framed by several points of view. As a consequence, damages escape the survey and many parts are lost in the model. As regards the construction materials and techniques, tools do not allow to take heterogeneities into account, which are very common in historic buildings. Moreover, as regards the working process, they are very time consuming. In fact, models have often such a number of points that they are unmanageable both by the computers and the users. All these drawbacks oblige the operator to check accurately the results of the survey and eventually to implement them by means of other non-destructive tests. This means that the critical interpretation of data by the operator is always indispensable.

2. Research aim

This study aims to evaluate the influence of the geometry in the structural assessment of architectural heritage, through the comparison of the results coming from the analysis of several 3D models which reproduce the same building element, but with a different level of detail.

3. Materials and methods

In order to argue the theme, it was chosen to focus the attention on the study of a column, which is a basic building element very common in architectural heritage, characterised by several parts variously moulded. It was chosen to refer to an existing case study, that is the monumental fountain in the middle of the eastern cloister of the former Monastery of Santa Maria in Gradi in Viterbo (Fig. 1). The monument is suitable for the purpose of the research, because it consists of eight slender columns linked by an entablature, having a similar geometry and a different damage pattern. The paper is organised in several parts which will be described above.

3.1. Analysis of the case study

In the first part of the paper, the monument is described according to the standard methodological approach used for architectural heritage [8], widely used in practice [9], that is by providing information about its history, geometry, construction technique and materials, past interventions and visible signs of damage. Historical notes come from bibliographical sources and from the inscriptions which is engraved on the monument itself. The geometric survey was conducted by using both analogic and digital metres (Leica Disto D2) and by following the triangulation and trilateration surveying methods. The construction materials and technique were surveyed by visible investigation, and the acquired information was supplemented by data coming from bibliography. Past interventions were reconstructed through the analysis of some historical photographs. The visible signs of damage were surveyed on site, and cracks depth was investigated through an ultrasonic (US) no-destructive test. The US system used consists on a Boviar Solgeo CMS pulsar-receiver and two piezoelectric transducers, a transmitting (TT) and a receiving (RT). The US pulse was 50 kHz. The depth of cracks was estimated by comparing the time-of-fly (t.o.f.) of the US wave, across the cracked and the uncracked parts of the element.

Fig. 1. The monumental fountain inside the Monastery of Santa Maria in Gradi in Viterbo.

3.2. The finite element model of the column

In the second part of the paper, the attention was paid on one among the eight columns that constitute the monument. A column with both deep and superficial cracks was chosen, in order to make some consideration about the relevance of this condition. The same element was modelled in 3D, in five ways which differs for the level of details. All virtual models were created with Autocad [10].

The structural analysis was done through a finite element approach, that is a technique widely used in architectural heritage. The finite element analysis (FEA) was conducted through Ansys Workbench, which is a general-purpose finite-element software [11]. The numerical representation of the column was done by adapting to this case the simplified micro-modelling strategy which is usually implemented for masonry [12]. According to this strategy, each unit that constitutes the building element is autonomous and is represented by solid elements, while interfaces are implemented through contact regions. Solid 186 elements (elements characterised by 20 nodes and having three degrees of freedom per node) were used to define the stone elements and the pins, while Contact 174 (3D surface-to-surface contact elements) were used to define the interfaces. A bonded contact behaviour was assigned to the contact regions. Cracks were modelled by subtraction of volumes. The entablature was not included in the model but its effect was indirectly considered by replacing it with a point mass element (Mass 21). The mesh was generated by using a hexahedron dominant method and a sizing control of 3 cm.

Next to the geometry modelling, construction materials were defined too. Because of the high artistic and historic value of the monument, no direct tests were carried out on the monument to estimate the mechanical features of its construction materials. For this reason, data used for the analysis were derived by literature.

3.3. Structural assessment of the selected building element

Finally, a comparison among the five models was done from a static and dynamic perspective, through the following analyses: static, buckling, modal and dynamic with response spectrum.

The first was conducted considering the structure subjected to its dead-load and an arbitrary 1 kN horizontal force. The models were constrained with fixed support, so that columns behaved as cantilever beams. The buckling phenomenon was studied by loading the five models with their own dead-load and with an arbitrary 1 kN axial force. Modal analysis was done by considering 25 eigenmodes, in order to involve more than the 90% of the total mass in all directions. The seismic performance was studied through a dynamic analysis with response spectrum. The approach consists of several phases, which are: the selection of the principal vibrational modes, the evaluation of the seismic action, the assessment of its effects on each mode, and their combination.

Seismic action was evaluated using the ground acceleration spectrum designed on the basis of the specifications contained in the National Italian Building Code and in the annex Explicative Document [13,14]. The basic seismic hazard of the site (lat. 42.413432, long. 12.112943) was defined through a maximum expected peak ground acceleration (ag) equal to 0.217 g, a maximum spectral amplification factor (F0) equal to 2.36 and a cut-off period for beginning of the constant velocity part of the spectrum (TC*) equal to 0.321 s. A Life Safety Limit State (SLV) was considered, with a consequent probability of exceedance (Pvr) of 10%. A nominal life (Vn) equal to 50 years, a class of use (Cv) equal to 2, and an occupancy category (Cu) equal to 1 were selected. The return period (Tr) associated to the SLV is equal to 475 years. The soil was classified as a ground type B (soft rocks) with topographic category T1 (flat land).

Thanks to these data, the acceleration spectrum was determined. It was applied in two orthogonal horizontal directions (the vertical contribution was ignored), and the results were variously combined considering ± 1 and ± 0.3 coefficients. Finally, the seismic effects were combined with those coming from the static analysis, in order to obtain the overall result.

Since the monument is made of a brittle material, the maximum load stress criterion (also known as Rankine criterion) was used to interpret data coming from the analysis. It consists in the comparison between the principal stress values in each element with the maximum admissible values of the material, both in tension and in compression.

4. The monumental fountain in the former Monastery of Santa Maria in Gradi in Viterbo

4.1. Architectural description of the monument

The column chosen to argue the theme of this study, belongs to a monumental fountain, which is in the centre of the southern cloister of the former Monastery of Santa Maria in Gradi, built between 1217 and 1243, now main centre of the Tuscia University [15]. The monument is an extraordinary example of Renaissance architecture in Viterbo [16]. The inscription engraved in the frieze of the entablature attests that it was built in the 1480, and defines it "fons amphiteatrumque", that is a fountain surrounded by a pergola. The latter consists of eight slender-stone columns surmounted by eight pieces of entablature which, as a whole, create an elegant fence. Geometric survey revealed that columns are 330 cm high and very slim, in comparison with composite-type columns designed according to the recommendations contained in Treatise on Architecture know at that time, such as the one wrote by Leon Battista Alberti [17]. In fact, the ratio between the height and the base-diameter of the shaft is 11/1 instead of 8–9/1, the base and the capital are 2/3 and 3/2 of the modulus, instead of 1/2 and 1/1 respectively, where the modulus is the lower diameter of the shaft, which in this case is 32 cm. Columns lay upon a cube-shaped pedestal with 50 cm sides. One among the faces of the pedestal is enriched by a moulded frame. The base of the column is decorated with two *torus* (convex, semi-circular moulding) and one *scotia* (concave moulding). The shaft (the highest element which constitutes the column) is plain and its diameter range from 29 cm to 32 cm because of the existence of the *entasis* (convex curve to the surface of the shaft). Capitals have different decorative motifs, all referable to Florentine models, very widespread in Viterbo [18]. However, they all have a *calathos* (inner-core of the capital), an *abacus* (the flat slab at the top of the capital) and four volutes. The entablature is 77 cm high and consists of an architrave with two bands on the outside, a plane frieze with the inscription carved in the internal side, and a moulded cornice. A plan of the monument is shown in Fig. 2(A). Here, the columns are labelled with capital letters from A to F, by following a clockwise order.

4.2. Construction techniques and materials

All the elements which constitute the monument are made of peperino stone which is the widespread construction material in Tuscia landscape (the ancient Etruria land which included North Latium, Umbria and Tuscany Italian regions), used in historic architectures above all from the Mediaeval Ages. Peperino is the common name used to identify a stone of volcanic origin which belongs to the group of Ignibriti (*Ignimbrite Cimina*). It was extracted from local quarries in Cimini Mounts, near Viterbo. The variety used in the monument has a grey colour and it is characterised by the presence of blackish impurities, that is mineral inclusions (feldspar, biotite, pyroxene) having a few millimetres diameter, embedded in the basaltic matrix [19].

The mechanical parameters of the stone were investigated by Berry and Sciotti [20], and they were referred to for this research. Mechanical tests were carried out by the scholars on some samples of stone variously oriented. They revealed that the material can be considered isotropic, despite the presence of the impurities. It is characterised by a unit weight of 2630 kg/m^3, a modulus of elasticity of 27,000 N/mm^2, a Poisson's ratio of 0.2, a uniaxial tensile and compressive strength of 2.16 N/mm^2 and 35.20 N/mm^2 respectively.

Because of its morphology (mineralogical composition, grain size and texture), the most important causes of degradation which

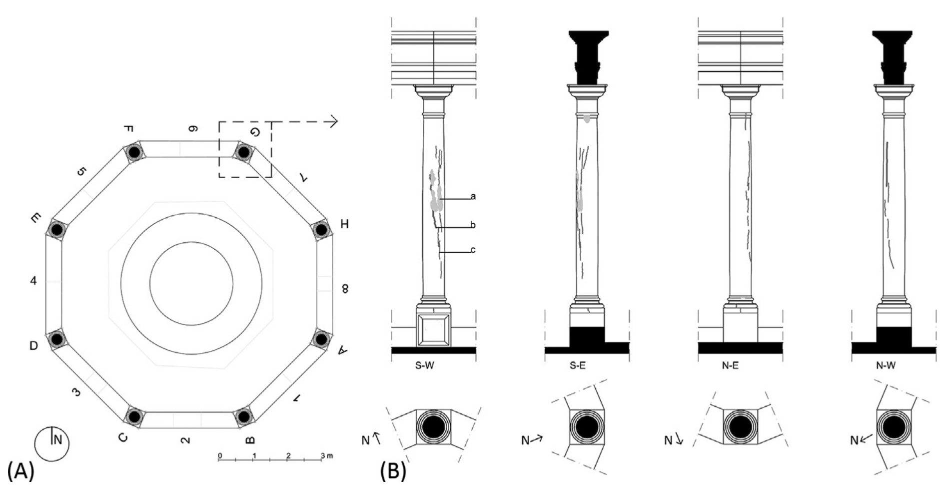

Fig. 2. (A) Plan of the fountain inside the former Monastery of Santa Maria in Gradi in Viterbo. Columns are sectioned at 0.70 m from the soil; (B) Map of the cracks in the column G. a: cementitious patches; b: major cracks (width >2 mm); c: minor cracks (width <2 mm).

affect this material are physical. In fact, they produce the weakening of the stone without changing the chemical structure [21]. Quick thermal changes, freeze-thaw cycles of the water which is into the pores of the stone, the crystallisation of the salts and the biodeterioration, contribute to the development of dangerous stresses in the outer layers of the material, which can produce micro-cracks, detachments and exfoliations.

As regards the construction technique, a visual inspection revealed that each column consists of several monolithic elements which not always coincide to the morphological parts of the architectonic element of the column as they are described in art history textbooks. These parts are: the plinth (the lower part of the base, which is prism-shaped), the upper part of the base (which is moulded), the shaft without the astragal that is part of the capital, the latter, the architrave, the frieze and the moulded cornice. The connecting elements had not been directly investigated, but it can be supposed that wrought iron pins were used to join the columns and the entablature parts. This hypothesis is supported by literature examples [22] and by the comparison with other local and coeval building elements directly investigable, such as some parts which belong to the ruined church of Santa Maria in Gradi (in the same architectural complex), destroyed during the Second World War and not yet reconstructed.

Mechanical properties of pre-industrial wrought iron are not easy to determine, as it was revealed by many scholars who dealt with this theme [23]. Some studies reveal that they are comparable to those of modern structural steel [24]. Values referred to in this study come from the Breymann's treatise on construction [25]. Wrought iron is characterised by a unit weight of 7788 kg/m^3, a modulus of elasticity of 196,133 N/mm^2, a Poisson's ratio of 0.3, a uniaxial tensile and compressive yield strength of 137.29 N/mm^2, a uniaxial tensile and compressive strength of 392.27 N/mm^2 and 343.23 N/mm^2 respectively.

4.3. Past damages and restoration interventions

From the end of the fifteenth, until the eighteenth century, not much information is known about interventions conducted on the former Monastery and on the fountain itself [26,27]. The earliest useful documents dealing with the monument date back to the beginning of the twentieth century, and consist of photographs and descriptions provided by Scriattoli [28] and Pinzi [29], two local historians, who recorded and denounced the degradation of the fountain and the architectural complex as a whole. In 1986 the local historian Carosi published some photographs aimed to record the inscription in the entablature [30]. They prove that a serious static problem affected the monument in the eighties, and that a scaffold (whose signs are still now visible) was installed to support the entablature and prevent its fall. In a photograph taken at the beginning of the nineties the scaffolder is no longer visible, because a restoration work was carried out meanwhile [31]. This intervention is proved by the existence of some invasive signs of mortar injections and cementitious patches, still now visible in several parts of the monument. Moreover, one of the columns was reinforced through three iron hoops, then removed.

4.4. Current damages

From an overview, the monument shows a lot of damage signs [32]. Some of these consist of the biological colonisation, which interest above all the shadowed parts, the encrustations, the exfoliation of the peperino stone, the expulsion of the grains which characterise the material, the absence of some little parts, above all in the bases and in the capitals, the presence of a lot of vertical cracks, perhaps due to the seismic events that interested the central regions of Italy from August 2016, and that lightly hit also the city of Viterbo in November of the same year.

Not all columns are equally damaged. Some of them do not show cracks or these are very little and smeared in the shaft. Some others show a high number of subvertical cracks whose thickness ranges from 1 to 2 mm, or exceptionally 3 mm.

Cracks depth were surveyed through an ultrasonic ND test conducted immediately after the seismic event. The survey revealed that the average velocity of the ultrasound wave measured on undamaged parts of the columns is 1504 m/s (std 85.25). To measure the depth of the cracks a pitch-catch setup was chosen [33], thus the transmitting and receiving transducers were put on the opposite sides of the crack itself. The average velocity of ultrasound waves is 2531.50 m/s (std 74.93) and 3361.57 m/s (std 227.21) in the case of small or wide cracks respectively. Such values allowed to estimate crack depth from 40 mm to 60 mm.

A detailed description of the crack pattern on each column is provided here after, while the map of the cracks in column G is showed in Fig. 2(B).

- Column A shows few subvertical cracks in the shaft, stretching from the capital to the base. The first torus, and the lower part of the base lack some parts. Cementitious patches are visible in the superior part of the shaft.
- Column B is the most damaged. A lot of crack is spread in the shaft. Some of them are in the boundary surface between the original stone and the cementitious patch. They are mainly due to

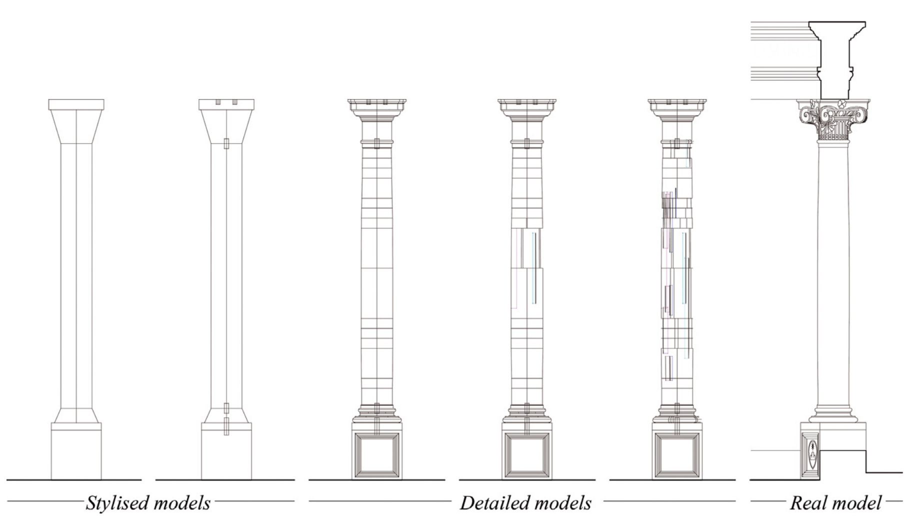

Fig. 3. Comparison between the five 3D models used for the FEA, and the architectonic 3D model (on the right).

Table 1
Main results of the static analysis.

Column model		1	2	3	4	5
Max displacement	mm	1.354	1.355	1.337	1.339	1.341
Max principal tension stress	N/mm^2	1.306	1.289	1.447	1.449	1.451
Max principal compression stress	N/mm^2	−2.456	−2.642	−2.639	−2.624	−2.609

1: stylised without pins; 2: stylised with pins; 3: detailed with pins; 4: detailed with pins and main cracks; 5: detailed with pins and all cracks.

the different thermal linear expansion coefficient of the concrete mortar ($1.12{\cdot}10^{-5}\,{}^{\circ}C^{-1}$) and the peperino stone ($4.30{\cdot}10^{-6}\,{}^{\circ}C^{-1}$).

- Column C shows a lot of small cracks spread in the shaft. The base lacks some parts.
- Column D shows very few cracks in the lower part of the shaft and it lacks some parts in the base.
- Column E shows few subvertical cracks in the shaft, stretching from the capital to the base. In the lower part one of the crack is about 2 mm width. The base has a crossing crack in the lower part and it lacks little parts in one torus.
- Column F shows few subvertical cracks in the shaft. The base has some crossing cracks in the lower parts and it lacks little parts in one torus, in the lower part of the base and in the superior part of the plinth.
- Column G shows spread subvertical cracks in the shaft, stretching from the capital to the base. The width of cracks ranges from less than 1 mm to about 2 mm. In the lower part of the base, a crossing crack is present too. Cementitious patches are visible in the central part of the shaft.
- Column H shows a lot of very small cracks spread in the shaft. A cementitious patch is visible in the plinth.

5. Geometric model of the selected column

According to the purpose of this study, column G was chosen among these that constitutes the monument. Since the width of cracks ranges from less than 1 mm to about 2 mm, it is possible to distinguish between small (minor than 1 mm) and wide (major than 2 mm) cracks, in order to made models that take only the latter or both of them into account. On the contrary, cementitious patches were omitted because their depth and adhesion to the stone were not characterised.

Column G was modelled in five ways, which differ in terms of detail and fidelity to the real object. The five models are reproduced in Fig. 3 and their features are described here after:

- Model 1; the column is widely simplified, and all its elements are reduced to several stylised geometric volumes; a cube for the pedestal, a truncated cone for the base and the capital, a cylinder for the shaft.
- Model 2; it is similar to the first but in this case, pins are introduced too, in order to reproduce the real construction technique. All pins are 3 cm square-shaped iron rebars. Pins are between the pedestal and the base (17 cm); the base and the shaft (10 cm); the shaft and the capital (10 cm).
- Model 3; the column shows all architectural details described in the first part of this paper, except for the capital. In this case, in fact, only the calathos and the abacus are modelled, while the volutes and all other decorative parts are omitted.
- Model 4; the previous model is completed with the principal cracks (2 mm width) which are in the shaft, in order to reproduce a simplified damaged geometric model. Cracks are modelled as subtracted volume. Each crack is like to a tiny slice 0.2 cm thick and 5.5 cm deep, while the length is variable.
- Model 5; the previous model is completed with all other minor cracks (minor than 2 mm width) which are in the shaft and in the base, in order to reproduce a complete damaged geometric model. As in the model 4, cracks are modelled as subtracted volume. Each crack is like to a tiny slice 0.1 cm thick and 5.0 cm deep.

6. The structural assessment

The comparison among the five models was made through the following analyses: static, buckling, modal and dynamic with response spectrum.

Data related to the static analysis are summarised in Table 1. In all the models, the maximum displacement occurs on the top of the capital, that is the free-end-of the element. Differences between values related to each model are on the order of the micron, so they are negligible.

As regards stress, all the values are far below those admissible for the materials, but some interesting differences exist between the stylised models and the detailed, in terms of range, location and stress patch. As regards the stylised models, the introduction of wrought iron-pins causes a reduction of the tensile stress (−1.30%) and an increase of the compression (+7.57%), due to the increase of the dead-load that reduce the effect of bending. Comparing the models 2 and 3, tensile stress increases of 12.26% while the compression decreases of 0.11%. This is due to the fact that the model 3 is lighter than the model 2, so the contribution of the dead-load is minor, and the effect of bending is amplified. Moreover, as it is shown in Fig. 4, in the former the maximum value is in the lower end of the shaft, while in the latter it is in the scotia (i.e. in the base) that is the smallest section of the geometric model. This is true also for the models 4 and 5. In these cases, as regard stress values, the maximum compressive stress is 0.57% and 1.14% lower in the model 4 and 5 than in the model 3, respectively, while the maximum tension stress is 0.14% and 0.27% higher. This effect is due to the different distribution of the mass due to the presence of the cracks in turn.

Results related to buckling are summarised in Table 2. As regards the stylised models, the critical load decreases slightly (0.05%) when the pins are taken into account. The same result occurs among the detailed models. The critical load in the models 4 and 5 is 0.12% and 0.46% lower than in the model 3, respectively. This result depends on the presence of the cracks which leads to the loss of the polar symmetry in the distribution of the mass of the element. Comparing the stylised and the detailed models on the whole, the critical load is lower in the former than in the latter. This is due to the different distribution of it along the height of the column itself. In fact, capitals are lighter in detailed models than in stylised, and the entasis causes a concentration of the mass in the lower part of the shaft.

As regards the modal analysis, the highest values of the participating masses in the three spatial direction, related to the vibration frequencies are summarised in Tables 3 and 4.

Modal analysis reveals that the first five natural frequencies are around 3, 55 and 79 Hz for all the five models, and that the principal vibrational frequencies (i.e. thus involving the higher percentage of mass) are around 3 and 79 Hz. The modal shape associated to the principal vibrational frequencies, related to each stylised and detailed model are shown in Figs. 5 and 6 respectively.

For all the models, a bending-torsional and an axial modal shape are associated to the natural frequencies that are around 3 Hz, and 79 Hz respectively. Because of the polar symmetry of the models,

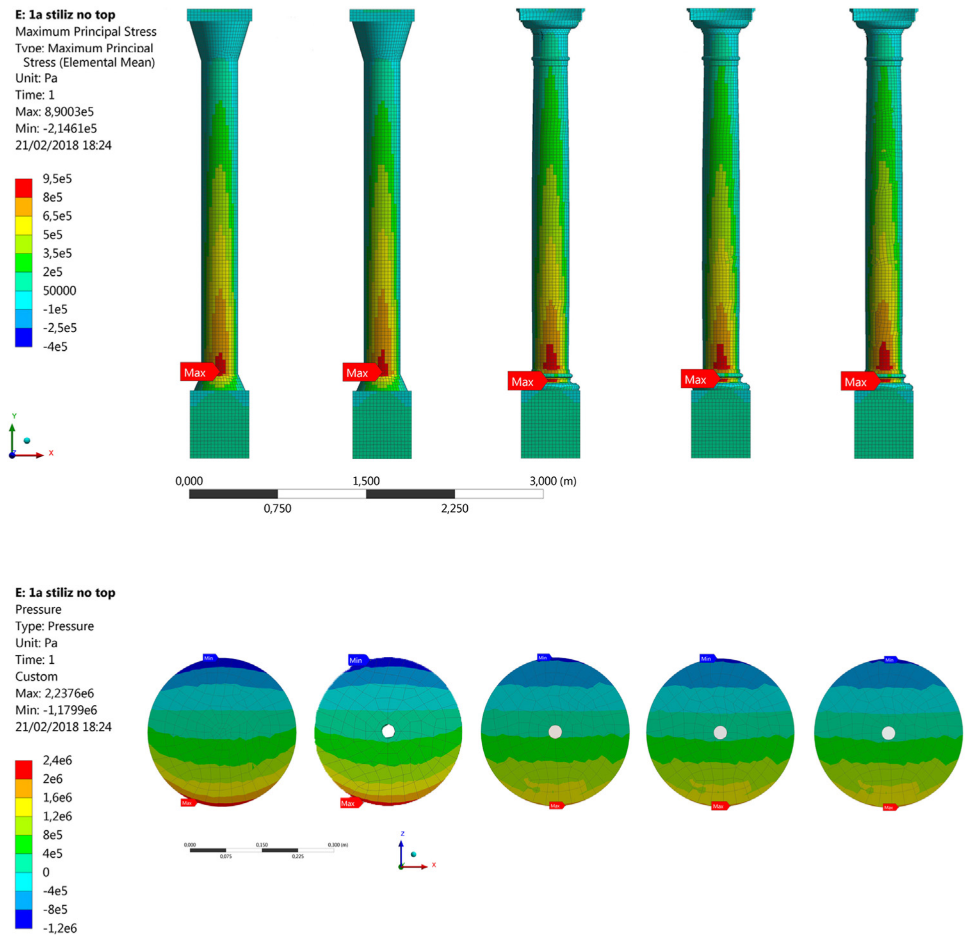

Fig. 4. Chart of the stress values in the column as a whole, and at the interface between the base and the shaft.

Table 2
Critical buckling load.

Column model		1	2	3	4	5
Y reaction component (Yrc)	kN	33.59	33.60	32.96	32.96	32.95
Load multiplier (LM)	–	112.61	112.51	118.61	118.47	118.10
Critical buckling load (LM × Yrc)	kN	3782.57	3780.34	3909.38	3904.77	3891.39

1: stylised without pins; 2: stylised with pins; 3: detailed with pins; 4: detailed with pins and main cracks; 5: detailed with pins and all cracks.

Table 3
Stylised models. Participating mass ratio, corresponding to the principal vibration frequencies.

	Freq. (Hz)	Participating mass (%)					
		X	*Y*	*Z*	Rot *X*	Rot *Y*	Rot *Z*
Model 1	3.31	68.34	0.00	10.84	13.43	7.30	84.69
	3.31	10.84	0.02	68.32	84.68	63.27	13.52
	54.93	0.00	4.10	5.41	1.16	2.78	0.02
	55.56	5.53	0.00	0.00	0.00	3.89	0.87
	79.65	0.00	79.33	0.02	0.26	0.11	0.45
	97.38	0.07	0.00	0.00	0.00	2.40	0.00
Model 2	3.31	79.15	0.00	0.00	0.01	29.00	98.20
	3.31	0.00	0.00	79.13	98.09	41.55	0.01
	54.90	0.00	4.08	5.41	1.16	2.79	0.02
	55.53	5.53	0.00	0.00	0.00	3.88	0.87
	79.72	0.00	79.34	0.02	0.25	0.11	0.45
	97.23	0.00	0.00	0.00	0.00	2.39	0.00

Freq.: vibrational frequency; *X* and *Z*: horizontal directions; *Y* vertical direction; Rot *X*: rotation around the *X* axis; Rot *Y*: rotation around the *Y* axis; Rot *Z*: rotation around the *Z* axis.

the values of the mass involved in modal shapes associated to the first four vibrational frequencies are coupled and alternate. In this case, the values of the vibrational frequencies are very close; the difference ranges from 0.00% to 1.15% and from 0.22 to 0.88% in the stylised and in the detailed models respectively. The introduction of the pins causes a significant increase of the percentage of mass associated to the vibrational frequencies. As regards the translation on the plane orthogonal to the *X* and the *Z* axes, it is 15.81% higher in the model 2 than in the model 1, while as regards the rotation around the *X* and *Z* axes it is 15.95% higher in the former than in the latter. On the contrary, the percentage of the mass associated to the translation along the *Y* axis is constant. The passage from the stylised model 2 to the detailed model 3, causes a negligible decrease of these values (ranging from 0.05% to 0.55%) and a change of the vibrational frequencies (+2.45% for the first and the second, −1.39% for the fifth). These values are confirmed also in the other two detailed models. Moreover, the direction of the first and second modal shapes are exchanged because of the presence of the moulded frame (according to the coordinate system, it is in the plane orthogonal to the *Z* axis).

In the model 4, the presence of the principal cracks causes a small decrease of the percentage of the mass associated to all modal shapes. As regards the translation on the plane orthogonal to the

Table 4
Detailed models. Participating mass ratio, corresponding to the principal vibration frequencies.

	Freq. (Hz)	Participating mass (%)					
		X	*Y*	*Z*	Rot *X*	Rot *Y*	Rot *Z*
Model 3	3.39	0.00	0.02	78.69	98.05	78.66	0.00
	3.40	78.66	0.00	0.00	0.00	0.00	98.15
	53.97	0.00	4.68	5.59	1.221	5.59	0.026
	54.99	5.74	0.00	0.00	0.00	0.00	0.90
	78.63	0.00	77.73	0.28	0.23	0.279	0.43
	120.76	0.11	0.00	0.00	0.00	0.00	0.00
Model 4	3.39	0.44	0.02	78.22	97.51	45.96	0.57
	3.40	78.22	0.00	0.44	0.55	24.35	97.59
	53.96	0.00	4.66	5.58	1.20	2.93	0.24
	54.97	5.73	0.00	0.00	0.00	3.80	0.90
	78.61	0.00	77.72	0.28	0.23	0.14	0.44
	118.26	0.10	0.00	0.00	0.00	1.64	0.00
Model 5	3.39	7.70	0.02	70.97	88.46	60.34	9.68
	3.40	70.97	0.00	7.70	9.60	9.97	88.48
	53.93	0.00	4.63	5.58	1.20	2.92	0.02
	54.92	5.72	0.00	0.00	0.00	3.84	0.90
	78.56	0.00	77.78	0.28	0.23	0.14	0.44
	112.78	0.10	0.00	0.00	0.00	1.64	0.00

Freq.: vibrational frequency; *X* and *Z*: horizontal directions; *Y* vertical direction; Rot *X*: rotation around the *X* axis; Rot *Y*: rotation around the *Y* axis; Rot *Z*: rotation around the *Z* axis.

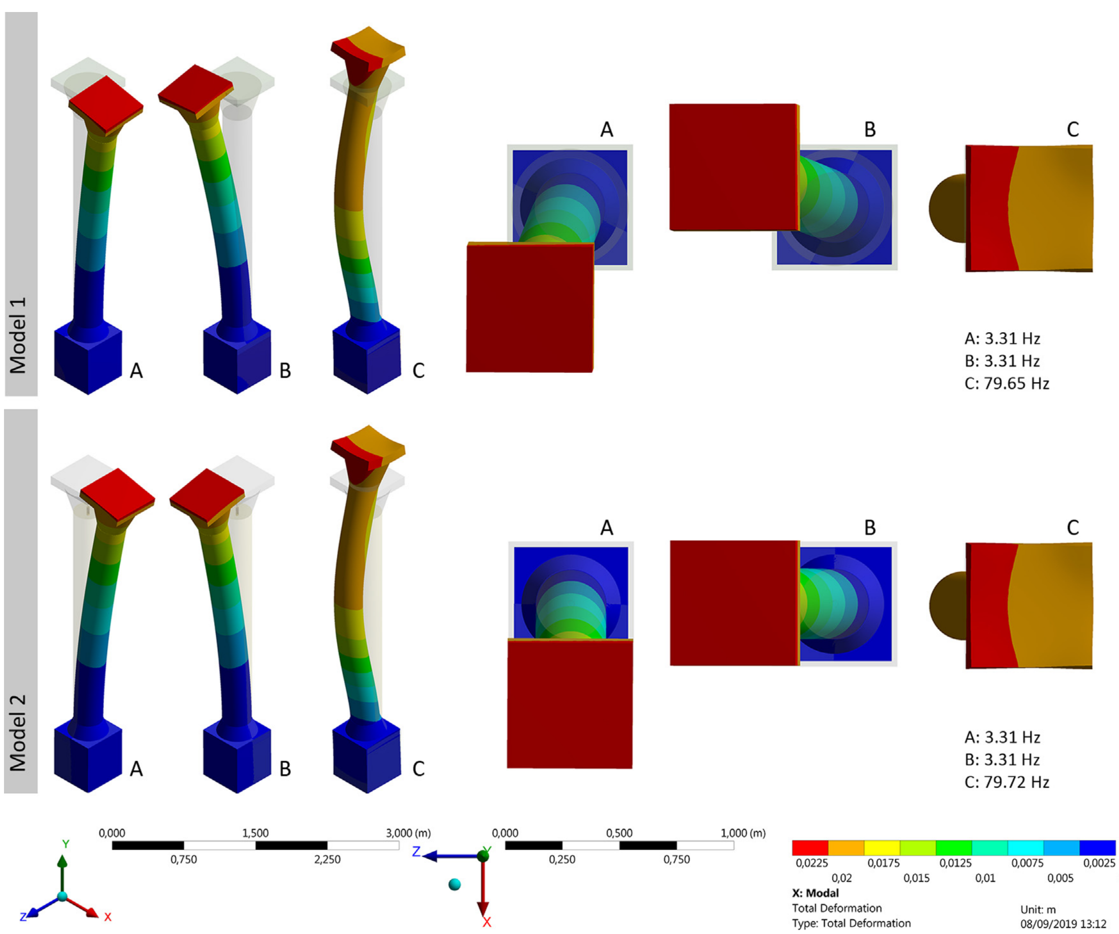

Fig. 5. Modal shapes related to the principal vibrational frequencies. Stylised models.

X and the *Z* axes, it is 0.60% lower than in the model 3, while as regards the rotation around the *X* and *Z* axes it is 0.57% lower. On the contrary, the percentage of the mass associated to torsion around the *Y* axis is significant. In the model 3, the 78.66% of the mass is involved in the first modal shape, while in the model 4, it is 45.96% in the first modal shape, and 24.35% in the second. In the model 5, the presence of all cracks causes a further significant decrease of the percentage of mass associated to all modal shapes. It is 9.78% lower than in the model 3 both in the case of translation on the plane orthogonal to the *X* and the *Z* axes, and rotation around the *X* and *Z* axes.

Regardless of the model, modal analysis revealed that the values of the principal vibrational frequencies are very close. For this reason, the seismic dynamic analysis was done by combining results of

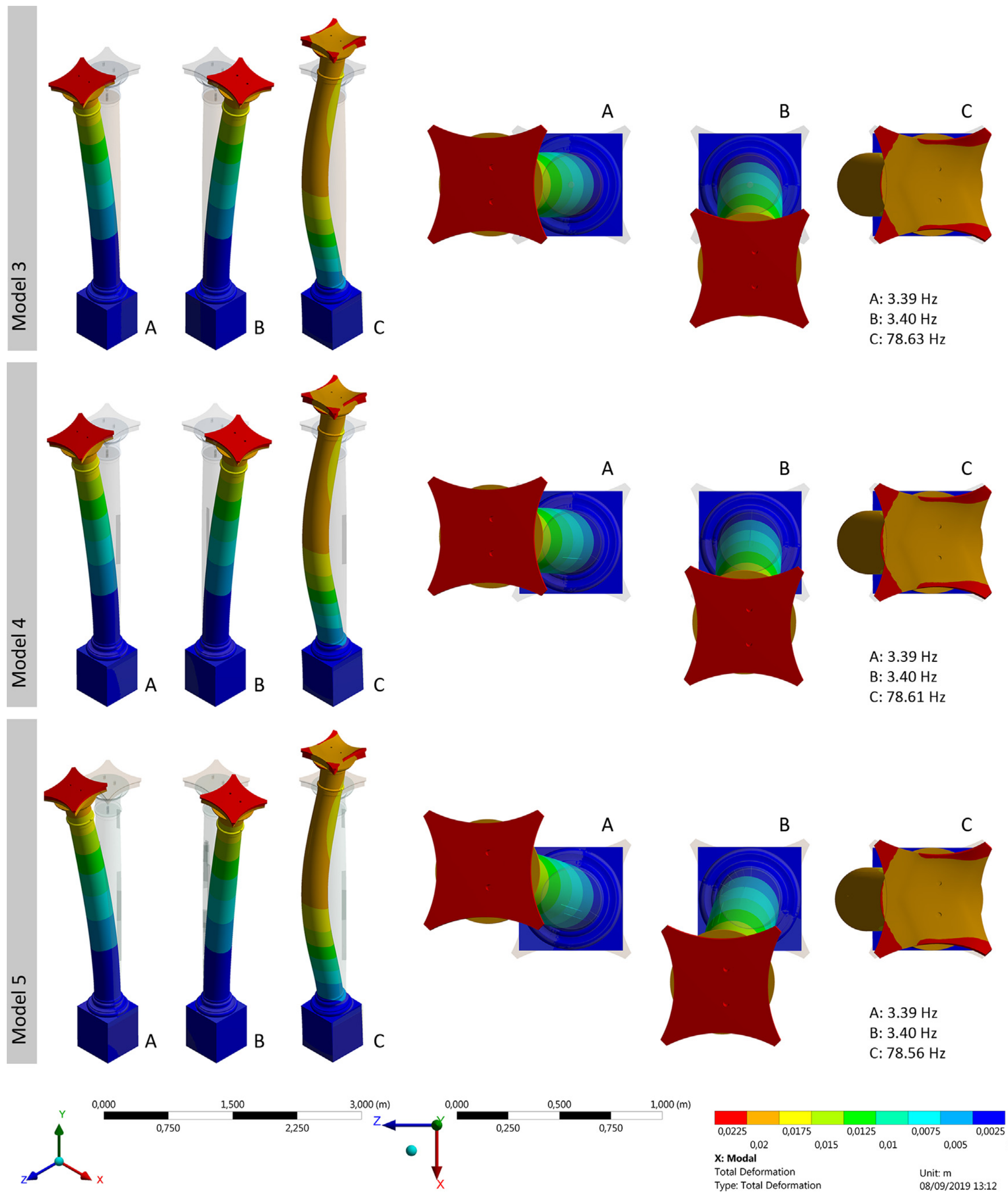

Fig. 6. Modal shapes related to the principal vibrational frequencies. Detailed models.

Table 5
Main results of the response spectrum analysis: maximum principal stress values (N/mm^2).

Load combination coefficients		Column model				
X axis	*Z* axis	1	2	3	4	5
+0.3	+1	25.482	24.752	24.543	24.550	24.556
−0.3	−1	−26.267	−25.098	−25.789	−25.791	−25.801

1: stylised without pins; 2: stylised with pins; 3: detailed with pins; 4: detailed with pins and main cracks; 5: detailed with pins and all cracks.

the modal analysis using a CQC (Complete quadratic combination) method. In such circumstances it is preferable because it takes the interaction of modes into account when these are closely spaced.

As regards the dynamic analysis, data related to the most serious load combinations, among those analysed, are summarised in Table 5. According to these, results coming from the static analysis are combined with the 30% and 100% of the results coming from the dynamic analysis, both in positive and negative directions (in relationship to the coordinate system).

The analysis reveals that the principal stresses are much higher in the detailed models than in the stylised. Values are around 25 N/mm^2 both in compression and in tension. In the first case they are always in the range of the admitted ultimate strength values for the stone material, while in the second they are much higher.

They could lead to the onset of new cracks if a new seismic event occurs.

As regards the two stylised models, tensile and compressive stress values differ for 2.95% and 4.66% respectively. Comparing the models 3 and 4, the tensile and compressive stress values differ for 0.84% and 2.75% respectively. When cracks are taken into accounts these values decrease but the difference is negligible. As regards their distribution, the maximum stresses are always in the bottom part of the shaft, in the case of the stylised models, and in the scotia (in the base), in the other cases, as in the static analysis.

7. Conclusions

The paper dealt with the influence of the geometric model on the structural analysis of a column.

The choice of a too much stylised model causes a wrong estimation of the volume, the mass, the stresses values and stress patches, and the modal shapes. By referring to the case study, the error between the model 1 (the most stylised) and the model 5 (the most detailed) is 4.8% in terms of volume, 2.0% in terms of mass, 6.2% and 11.1% in terms of compressive and tensile stress in static analysis, 1.8% and 3.8% in terms of compressive and tensile stress in dynamic analysis, 2.9% in terms of critical bucking load, 4.2% in terms of percentage of mass associated to the principal modal shapes.

Considering the real constructive technique is important for at least two reasons. Firstly, they allow to take into account the real unit weight and stiffness of the different materials which could exist in the element. Moreover, the case study reveals that when the real constructive technique is taken into account, a more careful estimation of the percentage of mass associated to the principal modal shapes comes out.

However, a stylised model which takes the constructive technic into account is still not sufficient. In fact, it allows neither to determine the true values of stresses, nor to locate the maximum values exactly. For this reason, a detailed model is to prefer.

Finally, also the damage assessment of the element is significant. In this study, the omission of cracks would cause the underestimation of the compression stresses in dynamic analysis, and tensile stresses in static analysis, that is dangerous in brittle materials like to stone.

In modal analysis, cracks influence the percentage of the mass which affect not only the bending but also the torsional deformation, despite the slenderness of the column.

Moreover, the case study reveals that the omission of the minor cracks leads to a negligible difference in terms of stresses but not in terms of bucking load and mass associated to the modal shapes.

Overall, the meaningful differences derived from the comparison of the results referred to all the models, suggests the importance to take care in the choice of the model, and in the implementation of results coming from other diagnostic tests, in a more complete and integrated strategic approach to the study and the assessment of the architectural heritage.

Funding

This work was supported by the STORM E.C. project H2020-DRS-11-2015, 700191.

Appendix A. Supplementary data

Supplementary material related to this article can be found, in the online version, at https://doi.org/10.1016/j.culher.2019.12.001.

References

[1] G. Boscato, E. Reccia, A. Cecchi, Non-destructive experimentation: dynamic identification of multi-leaf masonry walls damaged and consolidated, Compos. Part B: Eng. 133 (2017) 145–165.
[2] M. Wróblewska, Measurement methods of building structures deflections, in: E3S Web of Conferences 36, 2018, p. 02010.
[3] F. Sciarretta, F. Antonelli, F. Peron, S. Caniglia, Final outcomes on the multidisciplinary long-term monitoring and preservation state investigation on the medieval external Façades of Palazzo Ducale in Venice, Italy, J. Civil Struct. Health Monit. 8 (1) (2018) 111–133.
[4] U. Almac, I.P. Pekmezci, M. Ahunbay, Numerical analysis of historic structural elements using 3D point cloud data, Open Constr. Build. Technol. J. 10 (1) (2016) 233–245.
[5] G. Di Gregorio, D. Giaccone, A. Monteleone, The Roman amphitheater of Syracuse: a forgotten archaeological artifact, in: C. Gambardella (Ed.), Heritage Architecture Landesign focus on Conservation Regeneration Innovation, Le vie dei Mercanti, XI Forum Internazionale di Studi, La scuola di Pitagora editrice, Napoli, 2013, pp. 788–795.
[6] E. Uçkan, et al., Ongoing studies on Ephesus ancient theatre within the scope of safeguarding Cultural Heritage through technical and organizational resources management (STORM) project, in: 16th European Conference on Earthquake Engineering, Thessaloniki, June 18–21, 2018.
[7] D. Dominici, M. Alicandro, E. Rosciano, V. Massimi, Multiscale documentation and monitoring of L'Aquila historical Centre using UAV photogrammetry, Int. Arch. Photogramm. Remote Sens. Spat. Inf. Sci. 62 (5) (2017) 365–371, http://dx.doi.org/10.5194/isprs-archives-XLII-5-W1-365-2017.
[8] G. Carbonara, Restauro architettonico: principi e metodo, Mancosu Editore, Rome, 2012.
[9] G. Boscato, et al., Approach and methodology in understanding the structural behaviour of historic arch bridges through dynamic monitoring: the case of Rialto bridge in Venice, in: Proceedings of 34th IABSE Symposium, Venice, Italy, September 22–24, 2010.
[10] AUTODESK® Autocad educational (Release 2017), AUTODESK, Inc.
[11] ANSYS® Academic Research Mechanical (Release 18.0), ANSYS, Inc.
[12] P.B. Lourenço, Computational Strategies for Masonry Structures, Delft University Press, Delft, 1996, Ph.D. Thesis.
[13] Aggiornamento delle «Norme tecniche per le costruzioni». Public Law 17 January 2018, Gazzetta Ufficiale della Repubblica Italiana 42 (Suppl. ordinario no. 8) (2018).
[14] Istruzioni per l'applicazione dell'«Aggiornamento delle "Norme tecniche per le costruzioni"» di cui al decreto ministeriale 17 gennaio 2018, Public Law no. 7, 21 January 2019, Gazzetta Ufficiale della Repubblica Italiana 35 (Suppl. ordinario no. 5) (2019).
[15] M. Miglio (Ed.), Santa Maria in Gradi, Agresotti, Viterbo, 1996.
[16] E. Bentivoglio, S. Valtieri, Viterbo nel Rinascimento, GB EditoriA, Rome, 2012, pp. 371–379.
[17] Leon Battista Alberti, On the Art of Building in Ten Books, J. Rykwert, N. Leach, R. Tavernor (trans.), the MIT Press, Cambridge, 1988.
[18] S. Valtieri, Rinascimento a Viterbo: Bernardo Rossellino, L'architettura 196 (1972) 686–694.
[19] Pinzari, et al., Peperino & Basaltina, Consorzio Viterbo-export Amministrazione Provinciale di Viterbo, Agnesotti, Viterbo, 1986.
[20] P. Berry, M. Sciotti, I "Peperini" del Lazio", in: 1st International Congress on Exploitation of Industrial Minerals and Rocks, Turin, October 4–5–6, 1970.
[21] L. Lazzarini, M. Laurenzi Tabasso, Il restauro della pietra, CEDAM, Padua, 1986.
[22] J.P. Adam, Roman Building. Materials and Techniques, B.T. Batsford, London, 1994.
[23] M. Bellanova, A. Baggioli, B. Rivolta, R. Felicetti, A. Cornaggia, Metallurgical and mechanical characterization of the historical tie-rod of Duomo di Milano, in: G. Druissi, G. Biscontin (Eds.), Scienza e beni culturali – Metalli in architettura. Conoscenza, Conservazione, Innovazione, Arcadia Ricerche srl, Bressanone, 2015, pp. 23–34.
[24] C. Calderini, P. Piccardo, Experimental characterization of ancient metal tie-rods in historic masonry buildings, Int. J. Archit. Herit. 13 (9) (2019) 1–13, http://dx.doi.org/10.1080/15583058.2018.1563230.
[25] G.A. Breymann, Trattato generale di costruzioni civili con cenni speciali intorno alle costruzioni grandiose, 3rd ed., vol. 3: Costruzioni metalliche (costruzioni in ferro), Villardi, Milano, 1877, pp. 8.
[26] S.E. Anselmi, Nuovi contributi documentari alle vicende architettoniche di Santa Maria in Gradi a Viterbo tra XVIII e XIX secolo, Studi Romani. Rivista trimestrale dell'istituto nazionale di studi romani 53 (1–2) (2005) 161–185.
[27] R. Guiducci, Contributi d'archivio alla storia di Santa Maria dei Gradi, in: F.F. Gandolfo, M.T. Marsilia (Eds.), Il Barocco a Viterbo, atti del convegno (8–11 ottobre 1998), Quatrini, Viterbo, 2001, pp. 77–93.
[28] A. Sciattoli, Viterbo nei suoi monumenti, Capaccini, Rome, 1915–1920, pp. 331–337.
[29] C. Pinzi, I principali monumenti di Viterbo, Guida pel visitatore, 3th ed., Tip. Monarchi, Viterbo, 1905, pp. 143–145.
[30] A. Carosi, Le epigrafi medioevali di Viterbo, Agnesotti, Viterbo, 1986, pp. 146–147.
[31] A. Carosi, Il complesso conventuale di S. M. in Gradi di Viterbo dell'ordine dei padri domenicani, Camera di Commercio, Industria, Artigianato e Agricoltura di Viterbo, Viterbo, 1993.
[32] ICOMOS-ISCS, Illustrated glossary on stone deterioration patterns, English-French Version (2008), https://www.icomos.org/publications/monuments_and_sites/15/pdf/Monuments_and_Sites_15_ISCS_Glossary_Stone.pdf (accessed 23.06.19).
[33] L.W. Schmerr, An ultrasonic system, in: Fundamentals of Ultrasonic Nondestructive Evaluation: A Modeling Approach, Springer, New York, 2013, pp. 1–14.